BBA - Molecular Basis of Disease 1867 (2021) 166205

Contents lists available at ScienceDirect

BBA - Molecular Basis of Disease

journal homepage: www.elsevier.com/locate/bbadis

Analysis of cathepsin B and cathepsin L treatment to clear toxic lysosomal protein aggregates in neuronal ceroid lipofuscinosis

Alessandro Di Spiezio [a], André R.A. Marques [b], Lina Schmidt [a], Niklas Thießen [a], Lisa Gallwitz [a], Jens Fogh [c], Udo Bartsch [d], Paul Saftig [a,*]

[a] Institute of Biochemistry, Christian-Albrechts-University Kiel, 24118 Kiel, Germany
[b] Chronic Diseases Research Centre (CEDOC), Universidade NOVA de Lisboa, 1150-082 Lisbon, Portugal
[c] OrfoNeuro ApS, Lynge, Denmark
[d] Department of Ophthalmology, Experimental Opthalmology, University Medical Center Hamburg-Eppendorf, 20246 Hamburg, Germany

ARTICLE INFO

Keywords:
Cathepsin B
Cathepsin L
Cathepsin D
Neuronal ceroid lipofuscinosis 10
Bulk proteolysis
Enzyme replacement therapy

ABSTRACT

Proteolysis mediated by lysosomal cathepsin proteases maintains a physiological flow in autophagy, phagocytosis and endocytosis. Neuronal Ceroid Lipofuscinosis (NCL) is a childhood neurodegenerative disorder characterized by disturbed autophagic flow and pathological accumulation of proteins. We demonstrated a therapeutic clearance of protein aggregates after dosing NCL10 mice with recombinant human pro-cathepsin-D. Prompted by these results and speculating that cathepsins may act in a redundant and in an hierarchical manner we envisaged that a treatment with human recombinant cysteine proteases pro-cathepsin-L (proCTSL) and pro-cathepsin-B (proCTSB) could similarly be used to induce protein degradation. Both enzymes were taken up by mannose 6-phosphate receptor- and LRP-receptor-mediated endocytosis and processed to the lysosomal mature cathepsins. In murine NCL10 astrocytes an abnormal increase in LAMP1 and saposin expression was revealed. Although proCTSB application did not improve this phenotype, proCTSL treatment led to reduced saposin-C levels in this model as well as in an acute brain slice model. Intracerebral dosing in a NCL10 mouse model revealed cellular and lysosomal uptake of both enzymes. Only proCTSL mildly reduced saposin-C levels and attenuated reactive astrogliosis. Application of both proteases did not improve weight loss and mortality of mutant mice. Our data reveal that although recombinant lysosomal proteases can be efficiently delivered to neuronal lysosomes cysteine proteases are less efficient in protein aggregates clearance as compared to the cathepsin-D treatment. Our data including *in vitro* degradation assays support the idea that bulk proteolysis requires a hierarchical process in which both aspartyl and cysteine hydrolases play a role.

1. Introduction

Lysosomes are intracellular vesicles involved in protein degradation of biological macromolecules [1,2]. Material to be degraded reaches this compartment mainly through endocytosis, phagocytosis or autophagy. More than 60 acid hydrolases mediate degradation of such macromolecules and accelerate endocytic/autophagic flow [3]. The products of these hydrolytic reactions can leave the lysosome by specialized membrane transporters.

Among the enzymes present in the lysosomes, cathepsins represent a group of lysosomal proteases which are divided in three different subgroups based on the amino acids present within the active site: (i) aspartyl proteases (cathepsin D, E), (ii) cysteine proteases (cathepsin B, L, C) and iii) serine proteases (cathepsin A, G). Cathepsins are synthesized in the endoplasmic reticulum as inactive proforms. During transit to lysosomes they are proteolytically processed to mature forms which

Abbreviations: CTSD, cathepsin D; NCL, neuronal ceroid lipofuscinosis 10; Sap, saposins; SCMAS, subunit C of the mitochondrial ATPase; KO, knockout; CTSB, cathepsin B; CTSL, cathepsin L; HEK293, human embryonic kidney; EBNA, ebstein-barr virus nuclear antigen-1; HIS, polyhistidine; MEF, mouse embryonic fibroblasts; M6P, mannose-6-phosphate; RAP, receptor-associated protein; LRP, low density lipoprotein receptor-related protein; LAMP1, lysosomal-associated membrane protein 1; LC3, microtubule-associated protein 1A/1B-light chain 3; CNS, central nervous system; P1, post-natal day 1; Iba1, Ionized calcium binding adaptor molecule 1; GFAP, Glial fibrillary acidic protein; AD, Alzheimer's disease; PD, Parkinson's disease; wt, wildtype; FGF-2, fibroblast growth factor-2; EGF, epidermal growth factor; PBS, phosphate-buffered saline; PFA, paraformaldehyde; HRP, horseradish-peroxidase; PB, phosphate buffer; BSA, bovine serum albumin.

* Corresponding author at: Biochemisches Institut, Christian-Albrechts-Universität Kiel, Olshausenstr. 40, D-24098 Kiel, Germany.
E-mail address: psaftig@biochem.uni-kiel.de (P. Saftig).

https://doi.org/10.1016/j.bbadis.2021.166205
Received 24 March 2021; Received in revised form 11 June 2021; Accepted 22 June 2021
Available online 30 June 2021
0925-4439/© 2021 Elsevier B.V. This article is made available under the Elsevier license (http://www.elsevier.com/open-access/userlicense/1.0/).

become fully active in the lumen of the acidic lysosomes [4].

In particular, cathepsin D (CTSD), which is ubiquitously expressed, appears as one of the more important lysosomal proteases. Indeed, CTSD deficiency leads to a congenital neurodegenerative disease classified as Neuronal Ceroid Lipofuscinosis 10 (NCL10). NCL10 is characterized by an impaired autophagic flux associated with lysosomal accumulation of saposins (Sap), subunit C of the mitochondrial ATPase (SCMAS) and lipofuscin. Such aggregates lead to neuronal cell death associated with premature death in patients and a NCL10 mouse model [5–7].

Less severe phenotypes were found in cathepsin B and cathepsin L-deficient mice. Cathepsin B knockout (KO) mice do not show obvious pathological alterations under unchallenged conditions [8], while cathepsin L KO mice reveal a number of organ-specific phenotypes demonstrating that cathepsin L has an important functions in the heart [9], skin [10] thymus [11] and thyroid [12]. Cathepsin B/L double-deficient mice show many similarities with NCL10 mice including autophagic alterations, pathological protein accumulation in neurons and neuronal cell death. These mice are characterized by an early-onset

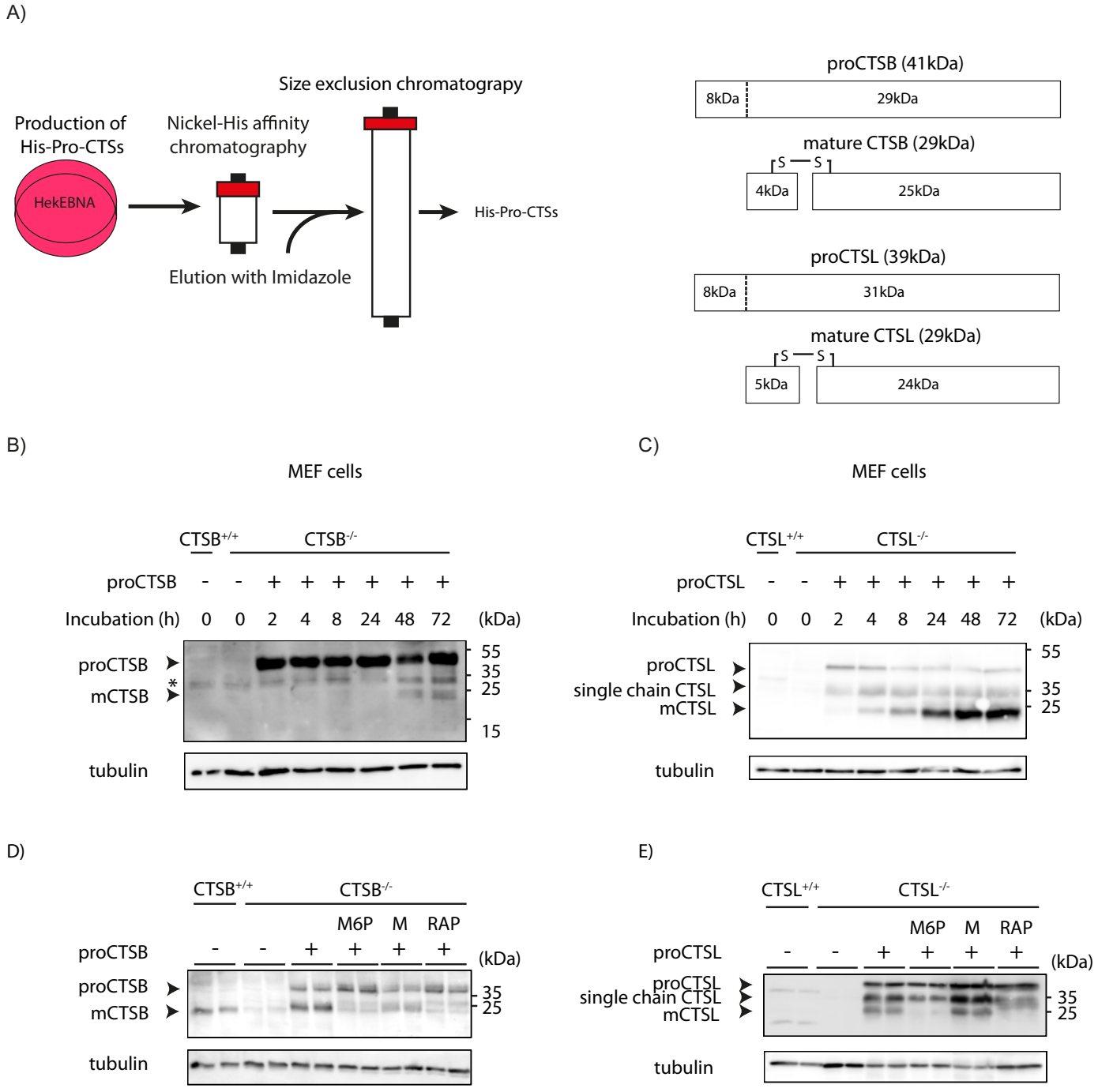

Fig. 1. Purification and *in vitro* testing of recombinant proCTSB and proCTSL. A) Left panel: schematic representation of the enzyme purification process. Right panel: maturation process of proCTSB and proCTSL. B) Immunoblot of CTSB KO MEF cells after incubation with 40 μg/mL of proCTSB for, 2 h, 4 h, 8 h, 24 h, 48 h, 72 h. C) Immunoblot of CTSL KO MEF cells after incubation with 40 μg/mL of proCTSL for 2 h, 4 h, 8 h, 24 h, 48 h, 72 h. D) Immunoblot of CTSB KO MEF cells after co-incubation of proCTSB with 40 mM mannose 6-phospate, 50 mM mannose and 750 nM RAP. E) Immunoblot of CTSL KO MEF cells after co-incubation of proCTSL with 40 mM mannose 6-phospate, 50 mM mannose and 750 nM RAP.

brain atrophy leading to lethality approximately four weeks after birth [13–15]. These observations and other studies suggest a significant degree of redundancy among the cathepsins [16–20].

In our previous study, we demonstrated that boosting lysosomal protein degradation by applying proCTSD is sufficient to clear protein aggregates resulting in reduced gliosis and neurodegeneration and an increased life span in the NCL10 preclinical model [21]. The rationale of our current study was to analyse in which way cathepsins can act in a redundant but also hierarchical manner. To this end we were interested if a single or combined application of the proforms of cathepsin B (proCTSB) and L (proCTSL) can be used to induce lysosomal degradation of protein aggregates.

2. Results

2.1. Production of recombinantly expressed proforms of human cathepsin B and cathepsin L

Human embryonic kidney (HEK293) Ebstein-Barr virus nuclear antigen-1 expressing (EBNA) cells were stably transfected to express either recombinant human proCTSB or proCTSL. A secretion signal peptide was inserted to drive the release of the recombinant proteins into the cell culture medium. ProCTSB or proCTSL were isolated from the medium by nickel affinity chromatography through the poly-histidine (His)-tag added to the enzyme's N-terminus. An additional size exclusion chromatography was used to obtain purified enzymes in PBS solution (Fig. 1A, left panel). The fractions resulting from the size exclusion chromatography were analysed by SDS-PAGE followed by Coomassie staining and western blot analysis. This analysis revealed a monomeric 41 kDa band corresponding to the size of proCTSB (Supplementary Fig. 1A, Fig. 1A right panel) and a 39 kDa band corresponding to the size of proCTSL (Supplementary Fig. 1B, Fig. 1A right panel). In addition, we observed the single chain CTSL (31 kDa) and mature CTSL (heavy chain 24 kDa) forms indicating that proCTSL partially undergoes auto-activation under neutral pH conditions (Fig. 1A right panel, Supplementary Fig. 1B).

Following these experimental procedures, we were able to obtain purified human proCTSB and proCTSL to study their potential therapeutic effect.

2.2. Cellular uptake of the recombinant cathepsin proteases

We were first interested to analyse the ability of cells to take up recombinant human proCTSB and proCTSL. Mouse embryonic fibroblasts (MEF) isolated from CTSB-deficient mice were incubated in the presence of recombinant proCTSB. Cellular uptake and intracellular processing of proCTSB were studied following time course of 2 h, 4 h, 8 h, 24 h, 48 h and 72 h (Fig. 1B). After 2 h incubation with 40 μg/mL of enzyme followed by cell lysis and immunoblot analysis, a band corresponding to proCTSB was revealed. It took another 48 h of incubation to detect the processed and mature form of CTSB (Fig. 1B, Supplementary Fig. 1C). Uptake experiments were also performed in human neuroblastoma cells SH-SY5Y. Using 40 μg/mL of enzyme for the incubation, SH-SY5Y CTSB knockout cells showed efficient uptake of proCTSB while mature CTSB was detected after 48 h in cell lysates (Supplementary Fig. 1D). A similar approach was used to evaluate the uptake of proCTSL in CTSL-deficient MEF cells (Fig. 1C, Supplementary Fig. 1C) and CTSL-deficient SH-SY5Y cells (Supplementary Fig. 1E). Also in this case knockout MEF cells were incubated in presence of 40 μg/mL proCTSL. The pro- and single chain CTSL were detectable in the cell lysate after 2 h of incubation. A gradual increase of the mature form of CTSL with time could also be observed, indicating the delivery of proCTSL to the lysosomal compartment (Fig. 1C, Supplementary Fig. 1C).

The uptake of lysosomal enzymes is mediated by specific receptors [22,23]. To analyse receptor-mediated endocytosis of proCTSB and proCTSL, a competition experiment was performed using: i) free mannose-6-phosphate (M6P) as competitor for the mannose-6-phosphate receptor, ii) mannose as a block of mannose-receptor mediated uptake and, iii) receptor-associated protein (RAP) as competitor of low density lipoprotein receptor-related protein (LRP) [24]. We applied exogenously proCTSB for 48 h and we observed that uptake and maturation was inhibited by both M6P and RAP protein in CTSB KO MEFs (Fig. 1D, Supplementary Fig. 1F). Similar experiment and results were obtained for proCTSL in CTSL KO MEFs (Fig. 1E, Supplementary Fig. 1G), suggesting that cathepsins follow similar mannose 6-phosphate receptor- and LRP-uptake routes towards the lysosomal compartment.

2.3. Protein aggregate clearance capacity after cathepsin application in astrocytes derived from NCL10 mice

Cathepsin D deficiency leads to impaired autophagy in humans and in animal models [5–7]. CTSD KO mice display progressive neurodegeneration and serve as a suitable model closely mimicking human NCL10 disease [7]. A hallmark of disease pathology is the cellular accumulation of undigested macromolecules forming toxic aggregation of proteins and hydrophobic molecules such as Saps, SCMAS and lipofuscin. To understand whether boosting proteolysis by application of pro-cathepsins is able to reduce such protein aggregates, we tested this approach in astrocytes derived from neural stem cells [25] from wildtype and CTSD KO mice. Neural stem cells from CTSD-deficient and wildtype mice were differentiated for two weeks into astrocytes. It is of note that unlike to neurons, neural stem cells-derived astrocytes can be cultivated for sufficient time to allow the development of a NCL-like storage phenotype. CTSD KO astrocytes were characterized by a significantly elevated number of clustered lysosomal-associated membrane protein 1 (LAMP1)-positive vesicles when compared to wildtype astrocytes (Fig. 2A, Supplementary Fig. 2). Moreover, immunostaining of CTSD KO astrocytes revealed lysosomes abnormally filled with SapD (Fig. 2B, Supplementary Fig. 2). The perinuclear lysosomal clusters present in the CTSD KO astrocytes were additionally characterized by significantly increased levels of SCMAS (Supplementary Fig. 3).

Immunoblot analysis confirmed that CTSD-deficient astrocytes presented increased LAMP1 and LC3II levels suggesting an impaired autophagy (Fig. 2C). An additional 1.7-fold increase of LAMP1, a 12-fold increase of SapC and a 3.5-fold increase of SapD were also detected by immunoblot in lysates from CTSD-deficient astrocytes when compared to lysates of wildtype astrocytes. Due to the strong increase in SapC levels in the following experiments we made use of this biomarker to evaluate the efficacy of cathepsin treatments (Fig. 2C). Altogether, we concluded that CTSD KO astrocytes are well suited to study the typical NCL10 cellular phenotype as observed *in vivo*.

To analyse if application of the pro-enzymes is able to reduce toxic protein aggregates, differentiated astrocytes were treated for 1 week with either 40 μg/mL of proCTSB, proCTSL or proCTSD. Immunoblot analysis revealed that proCTSB treatment was not able to reduce SapC accumulation, while proCTSD and proCTSL treatments was more efficient in clearance of SapC aggregates leading to respectively a ~70% and ~40% reduction compared to KO control astrocytes (Fig. 2D). Both LAMP1 and LC3II levels were only weakly reduced by proCTSB and proCTSL treatment compared to CTSD treatment (Fig. 2D and E). Remarkably, LAMP1 immunostaining showed that proCTSB treatment reduced lysosomal clustering and SCMAS/LAMP1 co-localization, while proCTSL treatment had an unexpected impact on the lysosomal morphology, *i.e.* leading to partially enlarged LAMP1 positive vesicles (Supplementary Fig. 3).

2.4. Clearance of protein aggregates in an ex vivo NCL10 model

We further tested the protein aggregate clearance capacity of proCTSB and proCTSL enzymes under *ex vivo* conditions. Organotypic brain slices were generated from 15 days old CTSD KO and wildtype mice. First, the capability to take up proCTSD in vibrosections was

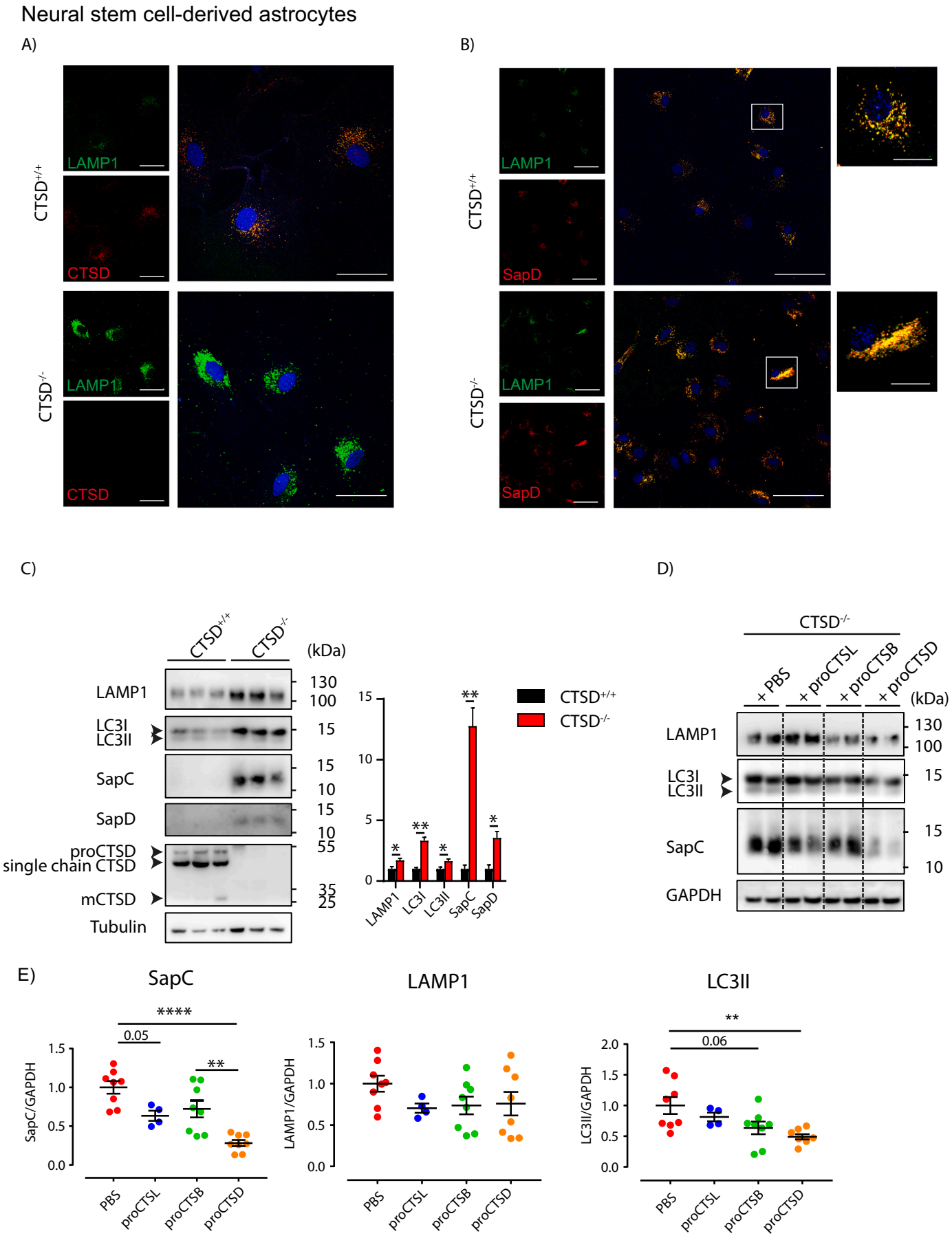

(caption on next page)

Fig. 2. Clearance of toxic protein aggregates *in vitro*. Immunostaining of neural stem cell-derived astrocytes from wildtype ($CTSD^{+/+}$) and CTSD KO ($CTSD^{-/-}$) mice. Co-staining of A) LAMP1 (lysosomal marker) and CTSD, B) LAMP1 and SapD (storage material marker). Scale bar 50 μm, scale bar insert 20 μm. C) Immunoblot and densitometry analysis of wildtype and CTSD KO astrocytes. D) Immunoblot analysis of astrocytes after 1 week of incubation with 40 μg/mL of proCTSB, proCTSL or proCTSD. E) Densitometry analysis of SapC, LAMP1 and LC3II of the immunoblot shown in panel D. Data ($n = 4$–8, mean ± S.E.M.) were analysed using one-way ANOVA followed by Tukey's *post hoc* comparisons test. * $P < 0.05$, ** $P < 0.01$, *** $P < 0.005$.

tested. To this end, we treated the sections for 2 weeks with recombinant human proCTSD (40 μg/mL) followed by immunostaining. Microscopy revealed that the enzyme was taken up by the brain slices and co-localized with LAMP1-positive lysosomes (Supplementary Fig. 4A). Immunoblot analysis revealed that in organotypic brain slices besides proCTSD also proCTSB and proCTSL were correctly processed into the corresponding mature and active forms (Supplementary Fig. 4B). Further characterization of these sections revealed that mock treated slices derived from the NCL10 mice showed an upregulation of LAMP1, p62, SapC and SCMAS compared to wildtype sections. ProCTSL treatment led to a 13% reduction of SapC and a 20% reduction of SCMAS compared to control vibrosections. ProCTSB treatment showed a 15% SapC reduction and a 26% reduction of SCMAS compared to control vibrosections (Supplementary Fig. 4C, D).

2.5. Dosing NCL10 mice with proCTSB and proCTSL

Since proCTSL treatment reduced SapC accumulation in NCL10 astrocytes and organotypic brain slices, we decided to dose NCL10 mice with recombinant human proCTSB and proCTSL and compared the therapeutic effect with mice treated with proCTSD [21]. First we asked whether mouse tissues are able to take up these recombinant enzymes. Cathepsin B- and cathepsin L-deficient mice were dosed intravenously with 50 mg/kg of proCTSB and 14 mg/kg of proCTSL, respectively. Twenty-four hours after injection, mice were sacrificed and brain and liver were harvested and analysed by immunoblot using specific anti human-CTSB and anti-human CTSL antibodies. Endogenous CTSB and CTSL were poorly detected due to the low cross-reactivity of the antibodies against mouse cysteine proteases. Livers of proCTSB and proCTSL injected mice were able to take up and process the recombinant enzymes correctly into the mature forms (Fig. 3A and B). However, both proCTSB and proCTSL were not able to cross the blood-brain barrier to reach the brain (Fig. 3A and B).

We therefore decided to intracranially deliver the enzymes to directly target the central nervous system (CNS). NCL10 mice were dosed with either proCTSB, proCTSL or as a comparison with proCTSD at post-natal day 1 (P1) and day 19 (P19). Mice were sacrificed 23 days after birth (Fig. 3C). Western blot analysis showed that both hydrolases were taken up in the brain (Fig. 3E and G), however, neither proCTSB nor proCTSL treatment were able to improve the body weight and prolong the lifespan of the NCL10 mice (Fig. 3C). Biochemical analysis of the brains revealed that proCTSB treatment resulted in a decreased LAMP1 and LC3II expression but did not reduce SapC accumulation (Fig. 3E and F). In contrast, proCTSL treatment did not reduce the LAMP1 levels. However, immunoblot of LC3II and SapC revealed a significant reduction of both proteins (LC3II: ~50%, SapC: ~30%) compared to the littermate control group (Fig. 3G and H).

To investigate if autophagy improvement after proCTSL treatment had an impact on the reported neuroinflammation [26–28], we performed IBA1/GFAP immunostaining [29,30] on brain sections from CTSD KO mice after proCTSB, proCTSL and proCTSD application. We could not observe any difference in the intensity of IBA1 or GFAP immunoreactivity between PBS treated controls and CTSD KO mice treated with proCTSB. However, proCTSL dosed mice showed a reduction of the GFAP-positive area (Fig. 4) which was also confirmed by immunoblot with a 18% reduction compared to the PBS injected NCL10 control. In mutant mice treated with CTSD reactive astrogliosis was clearly attenuated when compared with all other experimental groups (Fig. 4). Immunohistochemistry analysis did not reveal difference in cell death among neurons, astrocytes and glia cells (data not shown).

The *in vivo* dosing data show that in contrast to proCTSD treatment the application of proCTSB and proCTSL only mildly improved the pathology in the NCL10 model arguing that cysteine proteases cannot significantly contribute to the clearance of pathological protein accumulations in NCL.

2.6. In vitro cleavage assay reveals redundancy of cathepsin activities

In order to test if different combination of the proteases may impact the proteolytic activity we set up an *in vitro* cleavage assay. Recombinant proCTSD, proCTSB and proCTSL were auto-activated for 90 min at 37 °C at pH 4.5 (Fig. 5A) [31,32]. Fluorogenic substrates were used to test cathepsins activity after *in vitro* activation. Both CTSD and CTSL are characterized by a narrow activity peak at pH 4 and pH 4.5, respectively. In contrast, CTSB showed proteolytic activity from pH 7 to pH 4 (Supplementary Fig. 5). Since the lysosomal lumen is characterized by an acid environment, the cleavage assay was performed at pH 4.5. Therefore, increasing amount of activated enzymes was incubated for 30 min with fluorescence-conjugated bovine serum albumin (BSA). The assay revealed that 100 ng of CTSD or CTSL were able to reduce the intensity of the 100 kDa band by 50% and 65%, respectively (Fig. 5B). Corresponding with our previous results activated CTSB only showed minor BSA cleavage capacity compared to the other two enzymes. Importantly, CTSD proteolytic activity was inhibited using pepstatin A. Leupeptin was able to inhibit the cysteine hydrolases CTSB and CTSL (Fig. 5B). Using this experimental setting, a mixture of the different cathepsins and its ability to promote (the 100 kDa) albumin degradation was tested. Activated CTSL showed higher proteolytic activity towards the substrate compared to activated CTSB and activated CTSD. Co-incubation of CTSL and CTSB did not further increase BSA degradation. Importantly, the mixture of the three proteases had the strongest effect and led to an 80% decrease of the 100 kDa BSA band and the strongest appearance of an about 5 kDa product band (Fig. 5D). Interestingly, the combined application of CTSL, CTSB and CTSD caused a different albumin fragmentation pattern compared to the single cathepsin applications (Fig. 5C). These results suggest that CTSD and CTSL may have synergic effects in lysosomal bulk proteolysis and a combination treatment may be useful to further improve therapeutic efficacy.

3. Discussion

Despite high expression levels in neurons cathepsin B and cathepsin L single-deficient mice do not display an overt CNS phenotype. However, animals lacking both CTSB and CTSL present with a shortened lifespan associated with brain atrophy. Moreover, histological analysis revealed the abnormal presence of neuronal autophagic vacuoles, an accumulation of autofluorescence intracellular deposits and SCMAS in the brain of the double-deficient mice [13,14]. These are typical hallmarks reminiscent of NCL disease in general and specifically similar to the neuronal NCL10 disease phenotype (cathepsin D deficiency) suggesting a certain degree of redundancy among these cathepsins. A proteomic analysis of CTSB/CTSL-deficient mouse brain lysosomes revealed the accumulation of at least 19 lysosomal proteins underlining the importance of CTSB and CTSL in keeping neuronal homeostasis regulating autophagy [18]. This prompted our major hypothesis that next to cathepsin-D at least cathepsin-L and cathepsin-B cooperate to digest proteins substrates within neuronal lysosomes in the context of NCL disease. It should be noted that also mutations in other lysosomal proteases such as

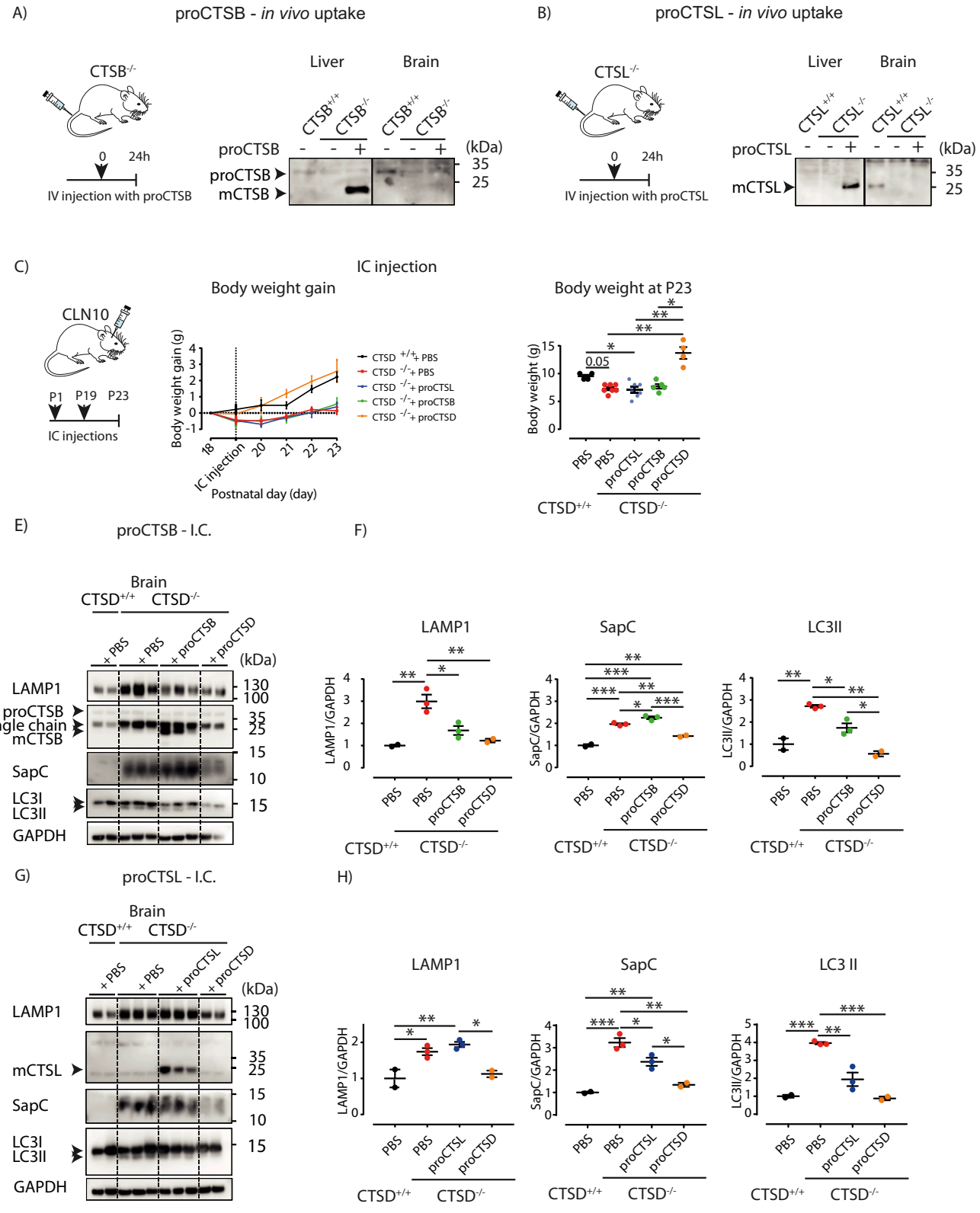

Fig. 3. *In vivo* testing and therapy in CLN10 mice. Uptake analysis of A) proCTSB and B) proCTSL in brain and liver of respective KO mice. C) left panel: intracranial dosing protocol in CLN10 mice. Mice were dosed at P1 and P19, to be then sacrificed at P23. C) middle panel: body weight gain development over time of wildtype and CLN10 mice dosed with proCTSB, proCTSL and proCTSD. C) Right panel: body weight of wildtype and CLN10 mice at P23. E) Immunoblot analysis of brains harvested from wildtype and CTSD KO mice. CTSD KO mice were injected with PBS, proCTSB or proCTSD. F) Densitometry analysis of LAMP1, LC3II and SapC of the immunoblot shown in panel E. Data ($n = 2–3$, mean ± S.E.M.) were analysed using an unpaired *t*-test. G) Immunoblot analysis of brains harvested from wildtype and CTSD KO mice. CTSD KO mice were injected with PBS, proCTSL or proCTSD. H) Densitometry analysis of LAMP1, LC3II and SapC of the immunoblot shown in panel G. Data (n = 2–3, mean ± S.E.M.) were analysed using one-way ANOVA followed by Tukey's *post hoc* comparisons test. * $P < 0.05$, ** $P < 0.01$, *** $P < 0.005$.

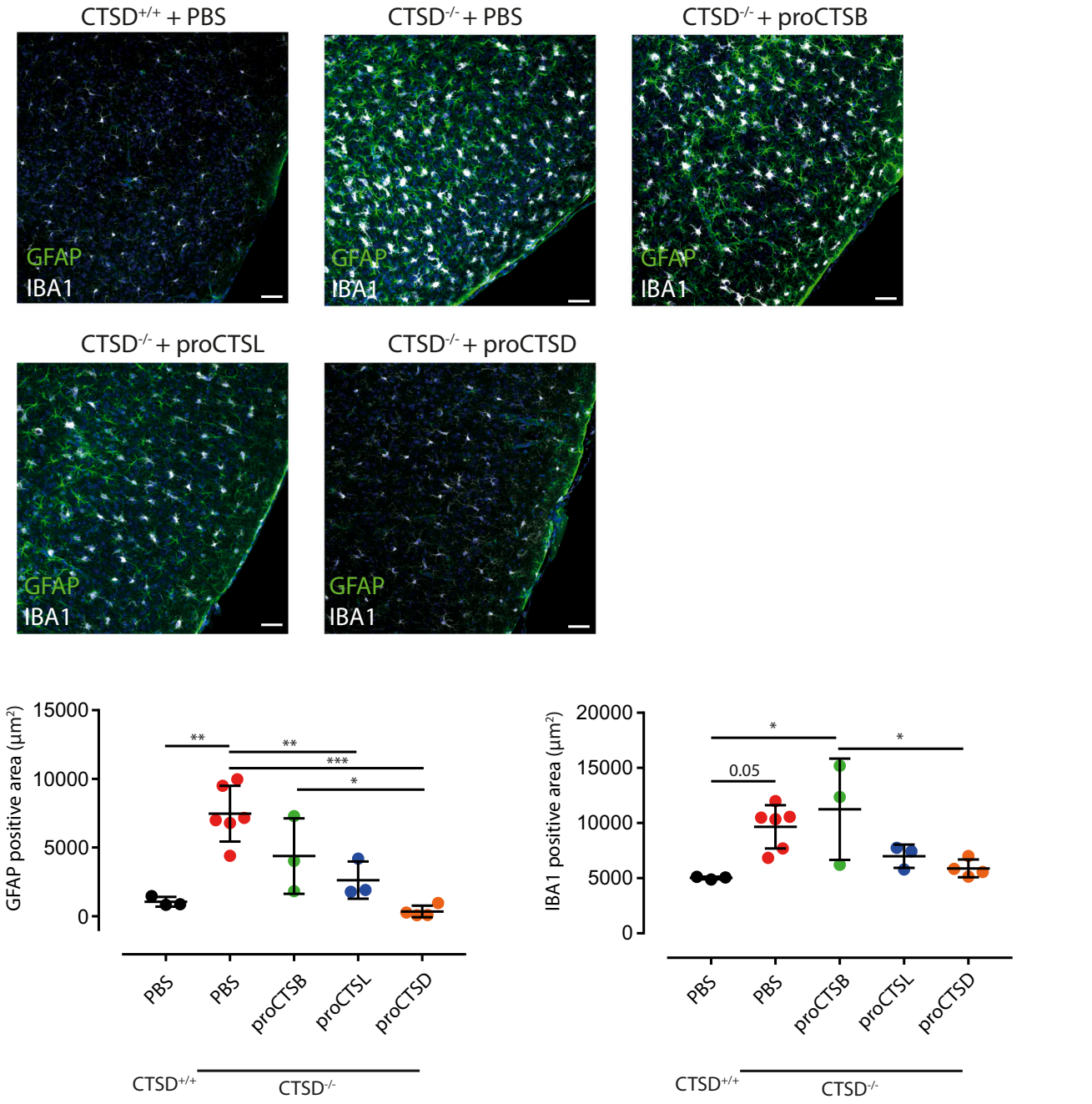

Fig. 4. proCTSL ameliorates astrogliosis and microgliosis in CLN10 mice. Immunohistochemistry of cortex of wildtype and CLN10 mice intracranially dosed with proCTSB, proCTSL or proCTSD. Co-staining of GFAP as marker for astrogliosis and IBA1 as marker for microgliosis. Scale bar: 50 µm. Comparison of GFAP- and IBA1-positive area detected by immunohistochemistry. Dots represent GFAP- or IBA1-positive area of single mouse. Data (n = 3–6, mean ± S.E.M.) were analysed using one-way ANOVA followed by Tukey's *post hoc* comparisons test. * $P < 0.05$, ** $P < 0.01$, *** $P < 0.005$.

tripeptidylpeptidase 1 (TPP1) and cathepsin-F are associated with different types of NCL, NCL2 and NCL13, respectively [33,34]. NCL2 and NCL13 patients are characterized by the typical lipofuscin and undigested protein accumulations.

In vitro studies applying different methods were performed to identify specific substrates or consensus motifs for both cathepsins. The glycine in position P3′ is the major determinant for CTSB endoprotease specificity. Moreover, CTSB shows a strong preference for glycine in position P1, a preference for aromatic and aliphatic amino acids in position P2 and for glycine, lysine, leucine and proline in P3. CTSL specificity is mainly guided by aromatic residues in position P2, while the enzyme displays mixed selectivity for glutamine and glycine in P1 [16,20,35]. From these studies it was concluded that cathepsins lack a robust substrate consensus motif defining the cleavage site. This may explain their rather broad range of specificity towards substrates and a major role in lysosomal bulk protein degradation was suggested [16,19,20,35].

Many neurodegenerative pathologies are characterized by the presence of intracellular misfolded protein aggregates. These are typical pathological cellular hallmarks in Alzheimer's disease (AD), Parkinson's disease (PD), Huntington disease, Prion disease and Batten (NCL) disease. For some of them, such as AD, PD and Prion disease, inducing autophagy was sufficient to ameliorate the pathological phenotype in mouse models of the diseases [36–38].

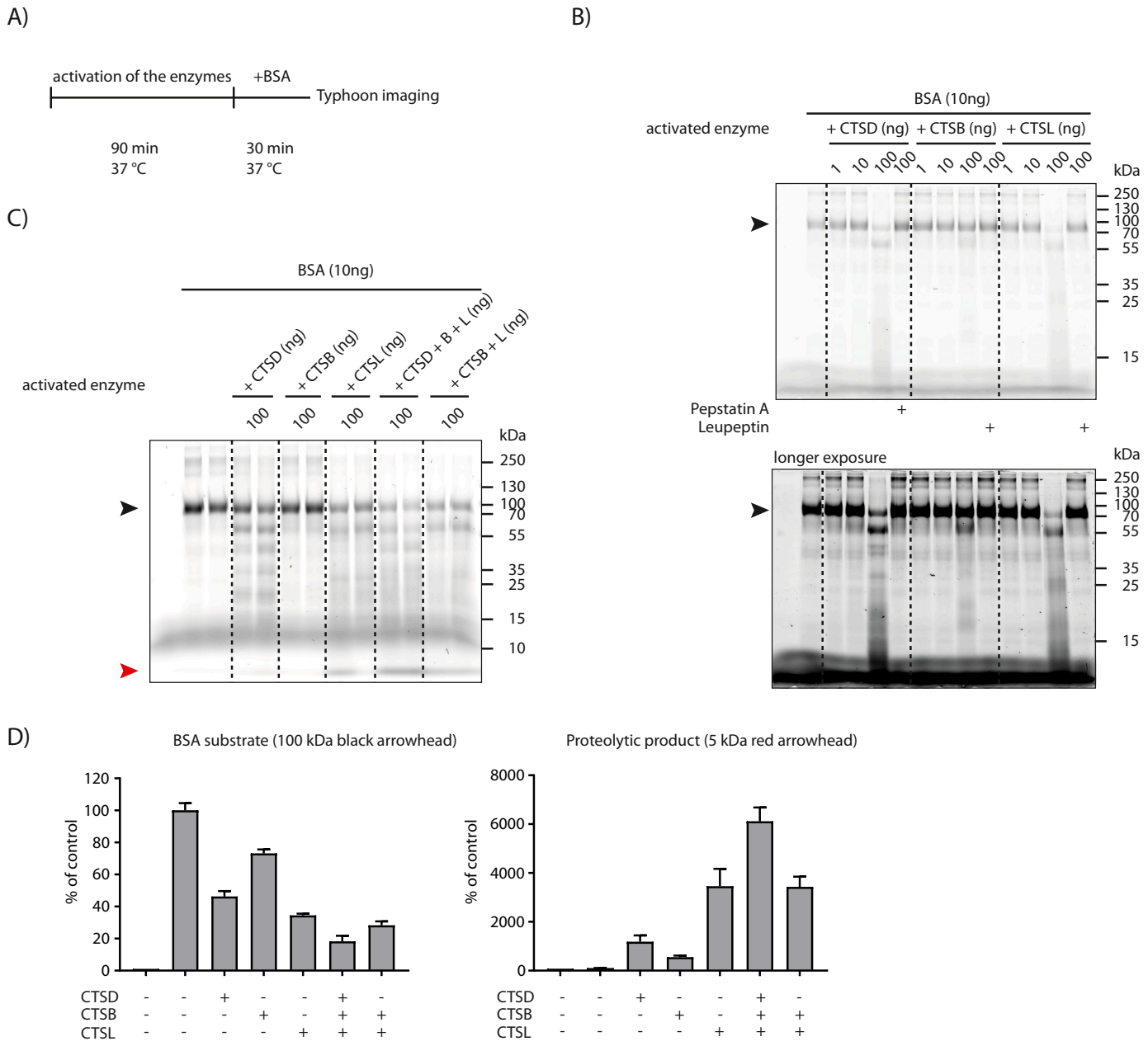

Fig. 5. CTSD and CTSL display a synergic effect in an *in vitro* albumin cleavage assay. A) Schematic representation of the cleavage assay pipeline. B) Bovine Serum albumin (BSA) cleavage assay with increasing amount of recombinant enzyme. Pepstatin A (360 μM) was used as a CTSD inhibitor, leupeptin (250 μM) was used as a combined inhibitor of CTSB and CTSL. C) BSA cleavage assay applying different types of protease cocktails and D) its quantification of the substrate and major product bands.

Enzyme replacement therapy was shown to be the most used approach to treat lysosomal storage disorders. Treatment with recombinant human TPP1 was approved for patients affected by CLN2. The patients dosed intraventricularly with the recombinant enzyme present less motor and language decline than historical controls, demonstrating the potential role of proteases in treating lysosomal storage disorders [39]. In our previous study, we demonstrated that intracranial enzyme replacement with recombinant human proCTSD was sufficient to prolong life span of a NCL10 mouse model, and to restore autophagic flux and lysosomal proteolytic processes [21]. We were therefore interested to examine the possibility to clear toxic protein aggregates by boosting lysosomal proteolysis using proCTSB and proCTSL. We were also interested to test the capability of these cysteine proteases to replace the necessity of an aspartyl hydrolase in lysosomal bulk proteolysis. NCL10 was chosen as a disease model due its rapid disease progression [5], its abundant presence of protein aggregates and the impaired autophagic flux in the CNS [6].

Our strategy was to first obtain sufficient recombinant catalytically inactive proCTSB and proCTSL. Like other lysosomal enzymes [4], also proCTSB and proCTSL appeared to be taken up by receptor-mediated endocytosis, however, proCTSB and proCTSL uptake and maturation showed some differences. ProCTSL maturation was 12 times faster as compared to the maturation of proCTSB. It has been previously suggested that proCTSB requires CTSD activity to be converted into the mature and active form, which might explain the slower rate of proCTSB maturation [40]. It was reported that proCTSL also requires CTSD activity for maturation [4], but apparently, in our system this did not seem to be crucial, as confirmed by the considerable amount of auto-

activation *in vitro*.

In accordance with our idea that also lysosomal cysteine proteinases can contribute to clearance of pathological storage in NCL we found that proCTSL treatment was capable to at least partially digest SapC-containing aggregates *in vitro* and *in vivo*. In contrast the application of proCTSB did not show such a beneficial proteolytic effect.

Despite similar subcellular localization, CTSL and CTSB exert different proteolytical activities. It was reported that CTSB has *exo-*, *endo-* and carboxydi-peptidase activity which works under different pH [41]. CTSB endopeptidase activity has an optimal pH between 4 and 6, while CTSB exo- and carboxydi-peptidase activity has a pH optimum of 6 [41]. This suggests that CTSB could work mainly as exopeptidase in the acidic lysosomal lumen. In contrast, CTSL shows an endopetidase activity similar to CTSD with an activity at an acidic pH optimum between 3.5 and 6.5 [42,43]. The biochemical similarity between CTSL and CTSD could explain the ability of CTSL to cleave SapC aggregates in cells and in the *in vivo* model, while such effect was not observed in CTSB treated cells and mice. Our *in vitro* assays assessing the cathepsin-mediated degradation of BSA revealed an efficient degradation capacity of CTSL and CTSD. CTSB was less efficient in degrading BSA. At least under these lysosome-like (pH 4.5) *in vitro* conditions the combined application of the three enzymes resulted in the most efficient degradative activity and an altered cleavage pattern. This indicates that cathepsins act in a sequential, redundant and coordinated manner.

3.1. Conclusion

Several studies showed that cathepsins have a wide range of substrates *in vitro* with overlapping specificity. However, our study indicates that there is a complex hierarchy of proteases acting within the lysosomal lumen. The partial SapC clearance achieved by CTSL means that the enzyme was biochemically able to cleave the peptide, however its activity was not sufficient to compensate for the missing aspartyl-protease degrading activity.

Further studies should focus on understanding the hierarchy and redundancy present among the cathepsins. This could give us valuable information necessary to develop targeted therapeutic strategies to treat disorders characterized by massive protein aggregation in the endocytic system and to improve an impaired autophagic flux by protease replacement strategies.

The notion that some enzymes could cooperate to digest certain substrates could lead to the use of a combination therapy applying aspartyl- and cysteine proteinases in parallel. This would bring the benefit of lowering the dosage of the therapeutic enzymes, thereby decreasing the risk of unwanted side effects.

4. Material and methods

4.1. Cathepsins cloning and purification

Cloning and purification of recombinant proCTSB and proCTSL are described in detail in the supplementary methods. Cloning and purification of recombinant proCTSD was performed as described previously [21].

4.2. Neural stem cell derived astrocytes

Neural stem cells were isolated as previously described [25]. In brief, neurospheres were generated from the cerebral cortex of 14-day-old wildtype (wt) and CTSD knockout (CTSD KO) mice with a standard protocol [44,45]. Once obtained, neurospheres were kept in culture for 2–3 passages, then enzymatically dissociated, and further cultivated under adherent conditions to obtain pure cultures of symmetrically dividing neural stem cells [46].

4.3. Immunostaining of astrocytes

Approximately 3×10^5 neural stem cells were seeded on 13 mm coverslips coated with 0.1% matrigel matrix (Corning) in a 12 well plate and cultivated in Dulbecco's modified Eagle's medium/F12 (DMEM/F12) supplemented with 1% B27, 1% N2 (both from Life Technologies), 10 ng/mL fibroblast growth factor-2 (FGF-2) and 10 ng/mL epidermal growth factor (EGF) (both from Immunotools). After 24 h medium was changed to a differentiation medium consisting of DMEM/F12 supplemented with 1% fetal bovine serum and 2% B27, and cells were further cultivated for 2 weeks during which neural stem cells differentiated into astrocytes. These astrocytes were treated with recombinant pro-enzymes (40 μg/mL of proCTSB, proCTSL or proCTSD) for 1 week in differentiation medium. After treatment with cathepsins, cells were washed 3 times with phosphate-buffered saline (PBS) and fixed with 4% paraformaldehyde (PFA). Astrocytes were incubated overnight with rabbit anti-CTSD (kindly provided by Prof. Andrej Hasilik, Münster, Germany), rat anti-LAMP1 (1D4B, DSHB), and rabbit anti-SapD (a kind gift from G. Grabowski from University of Cincinnati College of Medicine) antibodies diluted 1:750 in a blocking solution. Then, coverslips were incubated with fluorophore conjugated secondary antibodies (Alexa Fluor; Thermo Fisher Scientific), finally washed, embedded with mounting solution and analysed with an Olympus FV1000D Laser Scanning Confocal Microscope (model: FV10-292-115).

4.4. Immunostaining of tissue

Mouse brains were fixed in 4% PFA for 4 h to be subsequently washed in phosphate buffer (PB) at 4 °C overnight, immersed in 30% sucrose in PB, and stored at 4 °C. Sections (35 μm) were cut sagittally with a Leica SM 2000R sliding microtome (Leica Microsystems) with dry-ice cooling and stored in PB containing 0.02% (w/v) sodium azide. Floating slides were washed 3 times with PB, blocked and permeabilized 0.5% Triton X-100, 4% normal goat serum (Gibco) and incubated overnight with rabbit anti-IBA1 (GTX100042, GeneTex) and mouse anti-GFAP (G3893, Sigma) antibodies diluted 1:750 in a blocking solution. After 3 washing steps with 0.3% Triton X-100 in PB, sections were incubated with Alexa Fluor-conjugated secondary antibodies (A31573 Donkey anti-rabbit 647, A21203 Donkey anti-mouse 594, Thermo Fisher Scientific) for 3 h at room temperature, washed again 3 times in washing buffer, and finally coverslipped in Mowiol/DABCO.

4.5. Western blot

All studied cells (MEF cells, SH-SY5Y cells, astrocytes) were used for western blot analysis. In general, cells were washed 3 times with PBS and then collected in 500 μL PBS supplemented with 1× complete Protease Inhibitor Cocktail (Roche). Later, cells were centrifuged, supernatant was removed and pellets were lysed by shaking in 50 μL RIPA for 1 h at 4 °C. Mouse brains were homogenized in PBS with 0.1% (v:v) Triton X-100 containing protease inhibitor cocktail using 3 porcelain beads (PeqLab) in 2-mL screw-cap microcentrifuge tubes. Samples were crushed with a Precellys® 24 homogenizer (Bertin) set at 6 $m \cdot s^{-1}$ for 20 s, two times. Obtained cell and tissue lysates were cleared by centrifugation at 4 °C for 15 min at 12,000 ×*g* and protein concentrations were determined using the BCA method (Thermo Fisher Scientific, 23,225). Samples were denatured with 5× Laemmli buffer (50% (v/v) 1 M Tris-HCl, pH 6.8, 50% (v/v) 100% glycerol, 10% (w/v) DTT, 10% (w/v) SDS, 0.01% (w/v) bromophenol blue), boiled for 4 min at 100 °C and separated by electrophoresis on 12.5% (w/v) SDS-PAGE gel or NuPage gradient gel (Thermo Fisher Scientific, NP0336BOX) running continuously at 80 V. Then, proteins were transferred to a nitrocellulose membrane (Whatman, GE Healthcare, 10,426,994) using a semi−dry blotting. The membranes were blocked for 30 min with 5% dry milk in TBS-T (20 mM Tris/HCl pH 7.0, 150 mM NaCl, 0.1% (v/v) Tween® 20). The following primary antibodies were used: rat anti-LAMP1 (1D4B,

Developmental Studies Hybridoma Bank, Iowa City, IA, USA), rabbit anti-p62 (BHL-PW-9860, Enzo Life Science, Farmindale, NY, USA), goat anti-CTSD (AF1014, R&D Systems), mouse anti-tubulin (E7, DSHB), rabbit anti-GAPDH (sc-25778, Santa Cruz Biotechnology), rabbit anti-LC3 (PM036, MBL), rabbit anti-SapD (a kind gift from G. Grabowski from University of Cincinnati College of Medicine, USA), rabbit anti-SapC (Pineda Antibody, Service, Berlin), rabbit anti-SCMAS (a kind gift from E. Neufeld from University of California-Los Angeles, USA), goat anti-CTSB (AF953, R&D Systems) and goat anti-CTSL (AF952, R&D Systems). Afterwards, blots were washed with TBS-T for 30 min and incubated for 1 h at RT with secondary antibodies coupled to horseradish-peroxidase (HRP) (goat anti-rabbit HRP, rabbit anti-goat HRP, goat anti-mouse HRP, goat anti-rat HRP) in a blocking solution. Horseradish peroxidase activity was detected by ImageQuant™ LAS 680 (GEHealthcare) after incubation with Amersham ECL Advanced Western Blotting Detection kit (GE Healthcare, RPN2135).

4.6. Animal experiments

Animal handling and care were performed in agreement with the German animal welfare law according to the guidelines of the Christian-Albrechts-University of Kiel. Animal experiment was approved by the Ministry of Energy, Agriculture, the Environment and Rural Areas Schleswig-Holstein under the reference number V242–40536/2016 (81–6/16).

All mice were housed in individually ventilated cage (IVC) under a 12 h light/12 h dark cycle with free access to food (pellets by Sniff Spezialdiäten, V1534) and water. Mice cages were maintained in a room with a temperature between 19 and 22 °C and humidity of 45–60%. CTSD deficient mice (NCL10 model) were obtained from heterozygotes matings and genotyped as previously described [5]. CTSB- and CTSL-deficient mice were kindly provided by Prof Thomas Reinheckel from the University of Freiburg.

4.7. Intracranial injection

Intracranial injections were performed as previously described [21]. Both male and female mice were used for the experiments. Briefly, mice were genotyped at postnatal day 0 (P0). Wildtype or CTSD KO mice were selected, dosed at day P1 and P19 with PBS or recombinant enzymes and sacrificed at P23. Mice were anaesthetized with isoflurane (2% in oxygenated air) and kept on a warm plate for the whole procedure. For P1 injection 10 μl containing 100 μg of recombinant protease was injected into the cauda putamen (single injection in the right hemisphere), similar injection was performed at P19 (single injection in the left hemisphere) using a microsyringe (30 G) carrying a spacing devise with an injection depth of 1.15 mm over a period of 3 min. The injection of 10 μl of PBS at P1 and P19 did not affect body weight development or behaviour of the dosed mice. At P23 mice were anaesthetized by intraperitoneal injection of 10 mg/mL Ketamine (Bremer Pharma GmbH, 26706) and 6 mg/ml Rompun® (Bayer, KPOCCNU) in 0.9% (w/v) NaCl solution and transcardially perfused with phosphate buffer 0.1 M. Brains were harvested, the right hemispheres were fixed in 4% PFA and used for immunohistochemistry, while the left hemispheres were used for western blot analysis.

4.8. Bovine serum albumin (BSA) in vitro cleavage

Different amounts of pro enzymes were activated for 90 min at 37 °C in 20 μL processing buffer (0.1 M Tris-HCl, 3 mM EDTA, 5 mM Cysteine) at pH 4.5. Later, 10 ng of Alexa Fluor 647-conjugated BSA (A34785, Thermo Fisher) were incubated with the activated enzyme for 30 min at 37 °C. Reaction was stopped placing the samples on ice, samples were boiled for 4 min at 100 °C with 5× Laemmli buffer and separated by electrophoresis on 10% (w/v) SDS-PAGE gel. SDS-PAGE gels were analysed with Amersham™ Typhoon™ Biomolecular Imager.

4.9. Cathepsin activity assay

Cathepsin activity was tested incubating 400 ng of activated CTSD, CTSB and CTSL with activity buffer (50 mM sodium acetate (pH 5.5), 0.1 M NaCl, 1 mM EDTA, and 0.2% Triton X-100) containing either 10 μM of CTSD substrate (Enzo Life Sciences, P-145) or 20 μM cathepsin B substrate (Enzo Life Sciences, P137) or 20 μM cathepsin L substrate (Bachem, 4003379). The fluorescence was measured using a Synergy™ HT Multi-Detection microplate reader (exc: 360 nm; em: 440 nm, band pass 40).

4.10. Statistical analysis

Data are expressed as mean ± S.E.M. For statistical analysis one-way ANOVA was employed using GraphPad Prism 5 (Graph Pad Software, Inc., San Diego, USA): * $P < 0.05$; ** $P < 0.01$; *** $P < 0.001$; **** $P < 0.0001$.

Funding

This work was supported in part by the Deutsche Forschungsgemeinschaft (SFB877, A3, Z3).

Disclosure statement

An author of this publication (JF) is part of OrfoNeuro ApS, Denmark which is developing products related to research described in this publication.

CRediT authorship contribution statement

Conceptualization: A.D., A.M., P.S.; methodology, A.D., A.M., U.B.; investigation, A.D., A.M., L.S., N.T., L.G.; resources, A.D., J.F., U.B., P.S.; data curation, A.D., A.M., P.S.; Writing—Original draft preparation, A. D., P.S.; supervision, P.S.; project administration, M.S. and A.D.; funding acquisition, P.S. All authors have read and agreed to the published version of the manuscript.

Declaration of competing interest

An author of this publication (JF) is part of OrfoNeuro ApS, Denmark which is developing products related to research described in this publication.

Acknowledgments

We would like to thank Marlies Rusch and Nadja Peter for their crucial technical support, Elizabeth Neufeld for kindly providing the SCMAS antibody and Gregory Grabowski for the SapD antibodies and Thomas Braulke for the RAP peptide.

Appendix A. Supplementary data

Supplementary data to this article can be found online at https://doi.org/10.1016/j.bbadis.2021.166205.

References

[1] D.F. Bainton, The discovery of lysosomes, J. Cell Biol. 91 (1981) 66s–76s.
[2] P.C. Trivedi, J.J. Bartlett, T. Pulinilkunnil, Lysosomal biology and function: modern view of cellular debris bin, Cells 9 (2020).
[3] P. Saftig, J. Klumperman, Lysosome biogenesis and lysosomal membrane proteins: trafficking meets function, Nat. Rev. Mol. Cell Biol. 10 (2009) 623–635.
[4] N. Katunuma, Posttranslational processing and modification of cathepsins and cystatins, J. Signal Transduction 2010 (2010), 375345.
[5] P. Saftig, M. Hetman, W. Schmahl, K. Weber, L. Heine, H. Mossmann, A. Koster, B. Hess, M. Evers, K. von Figura, et al., Mice deficient for the lysosomal proteinase

cathepsin D exhibit progressive atrophy of the intestinal mucosa and profound destruction of lymphoid cells, EMBO J. 14 (1995) 3599–3608.
[6] M. Koike, H. Nakanishi, P. Saftig, J. Ezaki, K. Isahara, Y. Ohsawa, W. Schulz-Schaeffer, T. Watanabe, S. Waguri, S. Kametaka, M. Shibata, K. Yamamoto, E. Kominami, C. Peters, K. von Figura, Y. Uchiyama, Cathepsin D deficiency induces lysosomal storage with ceroid lipofuscin in mouse CNS neurons, J. Neurosci. 20 (2000) 6898–6906.
[7] R. Steinfeld, K. Reinhardt, K. Schreiber, M. Hillebrand, R. Kraetzner, W. Bruck, P. Saftig, J. Gartner, Cathepsin D deficiency is associated with a human neurodegenerative disorder, Am. J. Hum. Genet. 78 (2006) 988–998.
[8] T. Reinheckel, J. Deussing, W. Roth, C. Peters, Towards specific functions of lysosomal cysteine peptidases: phenotypes of mice deficient for cathepsin B or cathepsin L, Biol. Chem. 382 (2001) 735–741.
[9] Stypmann, Proc. Natl. Acad. Sci. USA, Proc. Natl. Acad. Sci. USA, 99 (2002) 6234.
[10] W. Roth, J. Deussing, V.A. Botchkarev, M. Pauly-Evers, P. Saftig, A. Hafner, P. Schmidt, W. Schmahl, J. Scherer, I. Anton-Lamprecht, K. Von Figura, R. Paus, C. Peters, Cathepsin L deficiency as molecular defect of furless: hyperproliferation of keratinocytes and pertubation of hair follicle cycling, FASEB J. 14 (2000) 2075–2086.
[11] T. Nakagawa, W. Roth, P. Wong, A. Nelson, A. Farr, J. Deussing, J.A. Villadangos, H. Ploegh, C. Peters, A.Y. Rudensky, Cathepsin L: critical role in Ii degradation and CD4 T cell selection in the thymus, Science (New York, N.Y.) 280 (1998) 450–453.
[12] B. Friedrichs, C. Tepel, T. Reinheckel, J. Deussing, K. von Figura, V. Herzog, C. Peters, P. Saftig, K. Brix, Thyroid functions of mouse cathepsins B, K, and L, J. Clin. Invest. 111 (2003) 1733–1745.
[13] M. Koike, M. Shibata, S. Waguri, K. Yoshimura, I. Tanida, E. Kominami, T. Gotow, C. Peters, K. von Figura, N. Mizushima, P. Saftig, Y. Uchiyama, Participation of autophagy in storage of lysosomes in neurons from mouse models of neuronal ceroid-lipofuscinoses (batten disease), Am. J. Pathol. 167 (2005) 1713–1728.
[14] U. Felbor, B. Kessler, W. Mothes, H.H. Goebel, H.L. Ploegh, R.T. Bronson, B. R. Olsen, Neuronal loss and brain atrophy in mice lacking cathepsins B and L, Proc. Natl. Acad. Sci. U. S. A. 99 (2002) 7883–7888.
[15] L. Sevenich, L.A. Pennacchio, C. Peters, T. Reinheckel, Human cathepsin L rescues the neurodegeneration and lethality in cathepsin B/L double-deficient mice, Biol. Chem. 387 (2006) 885–891.
[16] M.L. Biniossek, D.K. Nagler, C. Becker-Pauly, O. Schilling, Proteomic identification of protease cleavage sites characterizes prime and non-prime specificity of cysteine cathepsins B, L, and S, J. Proteome Res. 10 (2011) 5363–5373.
[17] A. Ciechanover, Proteolysis: from the lysosome to ubiquitin and the proteasome, Nat. Rev. Mol. Cell Biol. 6 (2005) 79–87.
[18] S. Stahl, Y. Reinders, E. Asan, W. Mothes, E. Conzelmann, A. Sickmann, U. Felbor, Proteomic analysis of cathepsin B- and L-deficient mouse brain lysosomes, Biochim. Biophys. Acta, 1774 (2007) 1237–1246.
[19] D. Arnold, W. Keilholz, H. Schild, T. Dumrese, S. Stevanovic, H.G. Rammensee, Substrate specificity of cathepsins D and E determined by N-terminal and C-terminal sequencing of peptide pools, Eur. J. Biochem. 249 (1997) 171–179.
[20] D.N. Gosalia, C.M. Salisbury, J.A. Ellman, S.L. Diamond, High throughput substrate specificity profiling of serine and cysteine proteases using solution-phase fluorogenic peptide microarrays, Mol. Cell. Proteomics 4 (2005) 626–636.
[21] A.R.A. Marques, A. Di Spiezio, N. Thiessen, L. Schmidt, J. Grotzinger, R. Lullmann-Rauch, M. Damme, S.E. Storck, C.U. Pietrzik, J. Fogh, J. Bar, M. Mikhaylova, M. Glatzel, M. Bassal, U. Bartsch, P. Saftig, Enzyme replacement therapy with recombinant pro-CTSD (cathepsin D) corrects defective proteolysis and autophagy in neuronal ceroid lipofuscinosis, Autophagy 16 (2020) 811–825.
[22] W.S. Sly, A. Kaplan, D.T. Achord, F.E. Brot, C.E. Bell, Receptor-mediated uptake of lysosomal enzymes, Prog. Clin. Biol. Res. 23 (1978) 547–551.
[23] O.C. Probst, P. Ton, B. Svoboda, A. Gannon, W. Schuhmann, J. Wieser, R. Pohlmann, L. Mach, The 46-kDa mannose 6-phosphate receptor does not depend on endosomal acidification for delivery of hydrolases to lysosomes, J. Cell Sci. 119 (2006) 4935–4943.
[24] T.E. Willnow, A. Rohlmann, J. Horton, H. Otani, J.R. Braun, R.E. Hammer, J. Herz, RAP, a specialized chaperone, prevents ligand-induced ER retention and degradation of LDL receptor-related endocytic receptors, EMBO J. 15 (1996) 2632–2639.
[25] G. Jung, J. Sun, B. Petrowitz, K. Riecken, K. Kruszewski, W. Jankowiak, F. Kunst, C. Skevas, G. Richard, B. Fehse, U. Bartsch, Genetically modified neural stem cells for a local and sustained delivery of neuroprotective factors to the dystrophic mouse retina, Stem Cells Transl. Med. 2 (2013) 1001–1010.
[26] A. Lopez, S.E. Lee, K. Wojta, E.M. Ramos, E. Klein, J. Chen, A.L. Boxer, M.L. Gorno-Tempini, D.H. Geschwind, L. Schlotawa, N.V. Ogryzko, E.H. Bigio, E. Rogalski, S. Weintraub, M.M. Mesulam, A. Fleming, G. Coppola, B.L. Miller, D. C. Rubinsztein, A152T tau allele causes neurodegeneration that can be ameliorated in a zebrafish model by autophagy induction, Brain J. Neurol. 140 (2017) 1128–1146.
[27] B.Z. Shao, B.Z. Han, Y.X. Zeng, D.F. Su, C. Liu, The roles of macrophage autophagy in atherosclerosis, Acta Pharmacol. Sin. 37 (2016) 150–156.
[28] M. Hassanpour, R. Rahbarghazi, M. Nouri, N. Aghamohammadzadeh, N. Safaei, M. Ahmadi, Role of autophagy in atherosclerosis: foe or friend? J. Inflamm. (London, England) 16 (2019) 8.
[29] D. Ito, Y. Imai, K. Ohsawa, K. Nakajima, Y. Fukuuchi, S. Kohsaka, Microglia-specific localisation of a novel calcium binding protein, Iba1, Brain Res. Mol. Brain Res. 57 (1998) 1–9.
[30] A. Bignami, D. Dahl, Specificity of the glial fibrillary acidic protein for astroglia, J. Histochem. Cytochem. 25 (1977) 466–469.
[31] J. Rozman, J. Stojan, R. Kuhelj, V. Turk, B. Turk, Autocatalytic processing of recombinant human procathepsin B is a bimolecular process, FEBS Lett. 459 (1999) 358–362.
[32] R. Ménard, E. Carmona, S. Takebe, E. Dufour, C. Plouffe, P. Mason, J.S. Mort, Autocatalytic processing of recombinant human procathepsin L. contribution of both intermolecular and unimolecular events in the processing of procathepsin L in vitro, J. Biol. Chem. 273 (1998) 4478–4484.
[33] K.R. Smith, H.H. Dahl, L. Canafoglia, E. Andermann, J. Damiano, M. Morbin, A. C. Bruni, G. Giaccone, P. Cossette, P. Saftig, J. Grötzinger, M. Schwake, F. Andermann, J.F. Staropoli, K.B. Sims, S.E. Mole, S. Franceschetti, N. A. Alexander, J.D. Cooper, H.A. Chapman, S. Carpenter, S.F. Berkovic, M. Bahlo, Cathepsin F mutations cause type B Kufs disease, an adult-onset neuronal ceroid lipofuscinosis, Hum. Mol. Genet. 22 (2013) 1417–1423.
[34] D.E. Sleat, R.J. Donnelly, H. Lackland, C.G. Liu, I. Sohar, R.K. Pullarkat, P. Lobel, Association of mutations in a lysosomal protein with classical late-infantile neuronal ceroid lipofuscinosis, Science (New York, N.Y.) 277 (1997) 1802–1805.
[35] R. Vidmar, M. Vizovisek, D. Turk, B. Turk, M. Fonovic, Protease cleavage site fingerprinting by label-free in-gel degradomics reveals pH-dependent specificity switch of legumain, EMBO J. 36 (2017) 2455–2465.
[36] Y. Aguib, A. Heiseke, S. Gilch, C. Riemer, M. Baier, H.M. Schatzl, A. Ertmer, Autophagy induction by trehalose counteracts cellular prion infection, Autophagy 5 (2009) 361–369.
[37] Q. He, J.B. Koprich, Y. Wang, W.B. Yu, B.G. Xiao, J.M. Brotchie, J. Wang, Treatment with trehalose prevents behavioral and neurochemical deficits produced in an AAV alpha-synuclein rat model of Parkinson's disease, Mol. Neurobiol. 53 (2016) 2258–2268.
[38] J. Du, Y. Liang, F. Xu, B. Sun, Z. Wang, Trehalose rescues Alzheimer's disease phenotypes in APP/PS1 transgenic mice, J. Pharm. Pharmacol. 65 (2013) 1753–1756.
[39] A. Schulz, T. Ajayi, N. Specchio, E. de Los Reyes, P. Gissen, D. Ballon, J.P. Dyke, H. Cahan, P. Slasor, D. Jacoby, A. Kohlschütter, Study of Intraventricular cerliponase Alfa for CLN2 disease, N. Engl. J. Med. 378 (2018) 1898–1907.
[40] A.A. Aghdassi, D.S. John, M. Sendler, F.U. Weiss, T. Reinheckel, J. Mayerle, M. M. Lerch, Cathepsin D regulates cathepsin B activation and disease severity predominantly in inflammatory cells during experimental pancreatitis, J. Biol. Chem. 293 (2018) 1018–1029.
[41] H. Koga, H. Yamada, Y. Nishimura, K. Kato, T. Imoto, Multiple proteolytic action of rat liver cathepsin B: specificities and pH-dependences of the endo- and exopeptidase activities, J. Biochem. 110 (1991) 179–188.
[42] D. Malagon, M. Diaz-Lopez, R. Benitez, F.J. Adroher, Cathepsin B- and L-like cysteine protease activities during the in vitro development of Hysterothylacium aduncum (Nematoda: Anisakidae), a worldwide fish parasite, Parasitol. Int. 59 (2010) 89–92.
[43] P. Briozzo, M. Morisset, F. Capony, C. Rougeot, H. Rochefort, In vitro degradation of extracellular matrix with Mr 52,000 cathepsin D secreted by breast cancer cells, Cancer Res. 48 (1988) 3688–3692.
[44] S. Pressmar, M. Ader, G. Richard, M. Schachner, U. Bartsch, The fate of heterotopically grafted neural precursor cells in the normal and dystrophic adult mouse retina, Invest. Ophthalmol. Vis. Sci. 42 (2001) 3311–3319.
[45] M. Ader, M. Schachner, U. Bartsch, Integration and differentiation of neural stem cells after transplantation into the dysmyelinated central nervous system of adult mice, Eur. J. Neurosci. 20 (2004) 1205–1210.
[46] L. Conti, S.M. Pollard, T. Gorba, E. Reitano, M. Toselli, G. Biella, Y. Sun, S. Sanzone, Q.L. Ying, E. Cattaneo, A. Smith, Niche-independent symmetrical self-renewal of a mammalian tissue stem cell, PLoS Biol. 3 (2005) e283.